

JPMTR 122 | 1904
DOI 10.14622/JPMTR-1904
UDC 005.31:774.8-021.465:004.356

Original scientific paper
Received: 2019-02-14
Accepted: 2019-05-16

A model for the prediction of print quality of a roll-to-roll inkjet press

Nicklas Norrick

Heidelberger Druckmaschinen AG,
Gutenbergring, 69168 Wiesloch, Germany

nicklas.norrick@heidelberg.com

Abstract

In this paper, a simulation model for the web dynamics of a digital label printing machine is presented and an exemplary application from practice is shown to verify the model. The basis is an extended modeling of the web dynamics including thermal effects in order to calculate the dynamic behavior of the continuous web. It is shown how thermal excitation can be used to measure the transfer function of the web dynamics and the influence of web tension control systems. Furthermore, a post-processing algorithm is presented which links the output data of the web dynamics simulation with the behavior of the inkjet printing data path and thus simulates digital inkjet printing. The results can be used to explain both registration errors from color to color as well as color density fluctuations within a raster image printed by a single color. As a practical example, a digital inkjet printing machine is considered in the following, in which a periodic variation in the color impression of a raster or solid surface can be recognized in the printed image. The fluctuation period corresponds to one revolution of the rotary encoder, which serves as a trigger signal for the inkjet printheads. With the help of the simulation model for the web dynamics and the presented post-processing algorithm, the origin of the error can be understood. Measurement and simulation are compared to verify the model. If the amplitude and the phase angle of the encoder error are measured, the print quality can be ensured by compensating the error within the inkjet printing data path. This is shown both in the simulation and on the basis of measured data.

Keywords: web dynamics, register, thermal effects, digital printing, transfer function

1. Introduction and background

Due to the consolidation of the printing press market in recent years and the requirement to be able to print small runs economically, there is an obvious shift from conventional printing processes, such as offset and gravure printing, to digital printing technology, especially inkjet printing. This trend applies equally to roll-to-roll and sheet-fed printing presses.

This new technology creates additional requirements for the modeling of machine dynamics, which takes into account the special effects that play a role and are different from classic impact printing processes. In this paper, we limit the consideration to roll-to-roll (web) presses.

The longitudinal dynamics of the web fundamentally influence the printing process and the achievable print quality. As a first approximation, the longitudinal

motion of the web can be decoupled from the transverse movement and movements perpendicular to the web's plane. For web presses, a plethora of publications dealing with the modeling of machine dynamics in the printing direction and the prediction of register and registration values exist. The first comprehensive process model was introduced in the 1970s in the pioneering work of Brandenburg (1971; 1976) and further developed by Whitworth and Harrison (1983). Further publications from various research groups around the world (Roisum, 1996; 1998; Wolfermann, 1995; Zitt, 2001; Galle, 2007; Yoshida, et. al, 2008; Schnabel, 2009) followed. Up to this day, this topic is of continued interest, as recent works show (Brandenburg, 2011; Göb, 2013; 2017; Seshadri, Pagilla and Lynch, 2013; Seshadri, Raul and Pagilla, 2014). The overall goal is always to most accurately control web tension, thereby optimizing the print quality. Overall, this increases productivity and reduces waste, which leads to the conservation of resources.

This paper presents a method for modeling and register simulation of roll-to-roll inkjet printing presses. In particular, it deals with the peculiarities of inkjet printing and presents a novel algorithm to calculate print quality from web dynamics simulations. The method is tested on a real case study. In this special case, it is considered how errors in the rotary encoder, which is used to clock the printheads, affect the print quality. In the process, simulation and measurement results are compared.

2. Methods and modeling

To model the web transport in longitudinal (printing) direction, the web is discretized into discrete web sections of the length l . Figure 1 shows a schematic of the control volume.

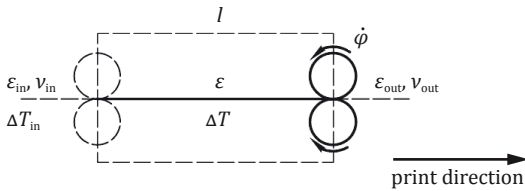


Figure 1: Schematic of the control volume for the derivation of the web transport equations where ϵ is strain, v is material flow, T is temperature and φ is phase shift

The web is assumed to be homogeneous, only stressed in longitudinal direction, massless and have negligible bending stiffness. The thickness of the web t is added to the radius of the rollers transporting the web yielding an effective radius r_{eff} . The width of the web is w . The control volume is bounded by a roller at the beginning and the end of the web section. For each section, the roller on the right side of the section is used for the formulation of the equation of conservation of angular momentum. The inputs to the web section are the web speed and strain.

For the following equations, the index $_{\text{in}}$ denotes values belonging to the preceding web section and the index $_{\text{out}}$ denotes values belonging to the following web section. Variables without an index belong to the web section in question.

From the continuity equation, the equation

$$\frac{d}{dt} \left(\frac{l}{1 + \epsilon} \right) = \frac{v_{\text{in}}}{1 + \epsilon_{\text{in}}} - \frac{v_{\text{out}}}{1 + \epsilon} \quad [1]$$

can be developed to describe the transport of web material in and out of the control volume, where v_{in} is the material flow into the web section with strain ϵ_{in} ,

v_{out} is the material flow out of the web section, and ϵ is the material strain in the web section. The material law for the web can be linear elastic with an elastic modulus E (Hooke's Law) or viscoelastic, for instance, a Kelvin-Voigt-model (Markert, 2013) to determine stress σ , of the form

$$\sigma = E\epsilon + R\dot{\epsilon} + E\alpha_T\Delta T \quad [2]$$

which also incorporates the strain of the material due to temperature effects (thermal expansion coefficient α_T) and the viscosity R . For paper, material parameters have been collected by Niskanen (2012). Generally speaking, it may be necessary to obtain the correct material parameters from measurements for each special case.

The equation of conservation of angular momentum for the roller on the right side of each web section yields

$$\theta\ddot{\varphi} + b\dot{\varphi} = M_{\text{out}} - M + M_{\text{drive}} + U \cos(\varphi + \delta) \quad [3]$$

The terms in this equation describe the torques M stemming from the web

$$M_{\text{out}} - M = (\sigma_{\text{out}} - \sigma) \cdot w_t r_{\text{eff}} \quad [4]$$

as well as a drive torque or friction torque M_{drive} as well as a sinusoidal unbalance torque with an amplitude U , phase shift φ and phase angle δ , at point w_t . The left-hand side of the equation is characterized by the moment of inertia of the roller θ and a linear damping coefficient b , which corresponds to a viscous damping component in the bearings.

The transport equation for the temperature of the web can be approximated by

$$\frac{d\Delta T}{dt} + \frac{v_{\text{in}} + v_{\text{out}}}{2} \frac{\Delta T - \Delta T_{\text{in}}}{l} = 0 \quad [5]$$

using an average temperature for each section as the mean between the temperature of the web coming into the section ΔT_{in} and the temperature leaving the section ΔT . This completes the equations for the web dynamics including thermal effects.

The system of nonlinear differential equations is transferred to the MATLAB®/Simulink® environment for simulation in the time domain.

For an arbitrary web section, this set of equations can be placed into a subsystem block with defined inputs and outputs. For each web section, a simulation block is required in which only a few parameters differ, so that it is very easy to build up a complete model of the web dynamics of a printing press with dozens of rollers.

In addition to the equations presented above, each block is configured to provide information as to whether the Euler-Eytelwein adhesion condition (Eytelwein, 2011) is met at the present time, as well as the bearing load for the web-carrying roller.

The model is used to answer fundamental questions about web dynamics, for example to determine the expected natural frequencies and mode shapes of the overall system as a function of the substrate elasticity, or to assist in the dimensioning of the drive motors. For detailed investigations with a direct relation to the achievable print quality, it is however necessary to extend this purely mechanical model by a register calculation algorithm, which will be detailed in the next section.

3. Register calculation algorithm

Inkjet printing is a non-impact printing process (NIP), meaning a printing process without a fixed image carrying device (Kipphan, 2000). An inkjet printhead is comprised of a multitude of tiny nozzles for the jetting of minute ink drops, each of which is responsible for one image pixel perpendicular to the printing direction. To print an image, the substrate is moved relative to the stationary printhead, so the resolution in the printing direction is defined by the printing speed and the jetting frequency. In order to achieve the high resolution a required for high print quality in transverse direction, the nozzles in the printhead are staggered, as shown schematically in Figure 2 for a fictitious printhead with $m = 4$ nozzle rows and $n = 7$ nozzle columns. A real printhead is of course made up of many more nozzles. Due to the staggered construction, the printing of a line in the transverse direction results in the situation that not all nozzles print at the same time but with a time delay. For constant speed printing, this does not matter, but changes in printing speed can create a sort of inter-head registration error which manifests itself as a color density variation in print direction.

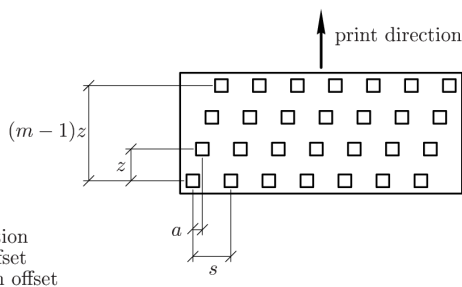


Figure 2: Schematic of the nozzle layout of an inkjet printhead

As a clock signal, a measuring system is required which accurately measures the current substrate speed. Typically, this signal is provided by a very accurate,

high-resolution rotary encoder. Due to signal propagation times, program run times and especially the flight time of the drop from head to substrate, the time delay between measured web speed or position and real substrate position upon impact of the ink drop on the substrate is not negligible.

The difficulties become clear with a numerical example to illustrate the order of magnitude: at 1200 dpi (equivalent to 21 μm resolution) and a print speed of 1 m/s, the printheads have a clock rate of 47 kHz. This means that every 21 μs a drop is triggered. With a drop speed of 5 m/s and a distance from printhead to substrate of 1 mm, the drop flight time is 200 μs .

In order to calculate the register between two printed dots, it is necessary to know the current position of a printed dot. That is, a reference point printed at a certain position must be tracked on its way through the machine. The difference between the position of the n -th printhead and the position of the reference point at time $t_p(n)$ (at this time the n -th printhead sets a new point) results in the registration error denoted as $1/n$.

In order to determine the current position of the reference point within a certain web section, the data of the actual angular velocities of the rollers and strains of the web sections are needed, but these are known from numerical simulation. To illustrate the derivation of the necessary equation, the sketch in Figure 3 is used. It shows the web at time $t_p(n)$ moving under two consecutive printheads, the first of which printed the reference point at an earlier point in time.

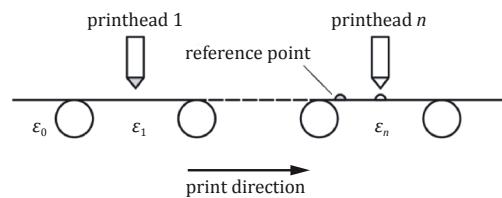


Figure 3: Sketch for the derivation of the point position

Let us consider section 1 with the corresponding strain ϵ_1 . First, it is necessary to determine the strain-free material length $dx_{\text{unstrained}}$ that has been transported from section 0 to section 1 in the time period from t_1 to \tilde{t} . With the generally valid formulas $v = dx/dt$ and $\epsilon = du/dx$ we can represent $dx_{\text{unstrained}}$ in the form

$$dx_{\text{unstrained}} = \frac{v_1(\tilde{t})}{1 + \epsilon_0(\tilde{t})} d\tilde{t} \tag{6}$$

Integration then leads us to the strain-free length transported into the section

$$x_{\text{unstrained}}(t) = \int_{t_1}^t \frac{v_1(\tilde{t})}{1 + \epsilon_0(\tilde{t})} d\tilde{t} \tag{7}$$

at the point in time t . The strain-free length $l_{\text{unstrained}}$ is the material length that was already present at the beginning between the printed point 1 and roller 1 at time t_i . The position of the point l_p at a point in time t taking into account the strain $\varepsilon_1(t)$ is then calculated by

$$l_p = (x_{\text{unstrained}}(t) + l_{\text{unstrained}})(1 + \varepsilon_1(t)) \quad [8]$$

At a second point in time t_2 , point 1 has traversed the first web section where $x = l_1$. The formula for a generalized section i is thus

$$x_{\text{unstrained}}(t) = \int_{t_i}^t \frac{v_i(\bar{t})}{1 + \varepsilon_{i-1}(\bar{t})} d\bar{t} \cdot (1 + \varepsilon_1(t)) + \sum_{l_i}^{l_{i-1}} l_j \quad [9]$$

wherein l_j are the lengths of the preceding web sections.

From the simulated encoder signal including the aforementioned time delay, the times are determined at which the web would have covered the distance from printhead 1 to printhead 2 without consideration of elongation effects. With these times, the difference between the location of point 1 at time t_2 and the location of the n -th printhead can be calculated – this is the registration error between the two points.

Algorithmically, this calculation was implemented as a MATLAB® script, with which a register prediction can be efficiently derived following a time-domain simulation of the web dynamics.

4. Results

The model just introduced is applied to an exemplary inkjet printing machine as shown schematically in Figure 4.

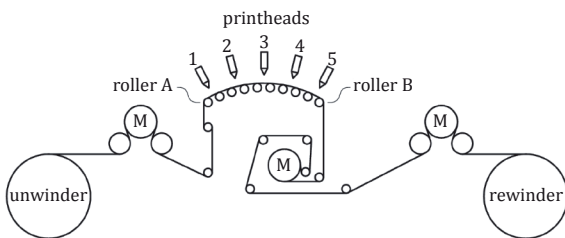


Figure 4: Schematic of a roll-to-roll inkjet printing press

The core of the machine is the digital printing unit with four process colors and white as a fifth color. The web is guided from an unwinder, past a web tensioning station over the so-called roller table, on which the substrate is guided over many small rollers past the printheads arranged one behind the other. The rotary encoder is mounted on the last roller of the roller table. The motors for web tension control are marked with M.

On the real machine, the web tension is measured on several rollers via flange-mounted force transducers. In the model, the web force sensors are integrated into each web section block as has been detailed in Section 2. In the model, the feedback control loop is closed via these virtual web force sensors. Overall, the model is made up of 31 discrete web sections.

As a plausibility check, a simulation result leading to comprehensible effects in the register is shown. For this purpose, it is prudent to switch off all other disturbing factors in the simulation (for example imbalances, errors on the unwinder, errors in the control system) and only a temperature step is initiated.

If heat is coupled into the web between the printing of two colors, for example due to a drying process, this leads to thermal expansion of the web. The subsequent web sections must run faster to maintain a constant web tension. The corresponding intermediate results for a temperature step ΔT at time $t = 10$ s are shown in Figure 5. It can be seen that the speed difference is very small. Nonetheless, this tiny difference in speed is what will lead to undesirable effects in the register.

Let us consider the register between the reference color (printhead 1) and a printhead n behind the heat input, while using a rotary encoder on roller A to clock the printheads. After the temperature step the register settles to a new stationary value which linearly increases with the distance of the printheads to each other, since the encoder is specifying an incorrect (too slow) speed. In the simulation, the thermal strain after the temperature step $\alpha_T \Delta T = 600 \mu\text{m}/\text{m}$ and is effective for the register 1/3 over a length of 500 mm and for the register 1/5 over a length of 1000 mm, resulting in a stationary registration error of 300 μm and 600 μm , respectively. The result is shown in Figure 6a.

Using the rotary encoder on roller B for clocking the printheads results in a different picture. Regardless of the distance of the printheads to each other, after a transient phase, a static offset occurs which is much smaller (20 %). This is the case since the web is only subjected to a deviation between real speed and the speed detected by the rotary encoder on a short subsection of the web path. The transient process in the register due to the step in web temperature can be interpreted as a superposition of the differences in strain and velocity in Figure 5. The situation can be seen in the Figure 6b.

An interesting phenomenon can be observed in the model – the temperature step excites vibrations in the web motion. With this knowledge, a quasi-harmonic excitation can be induced into the system by means of a printed pattern, e.g. zebra crossing stripes. For

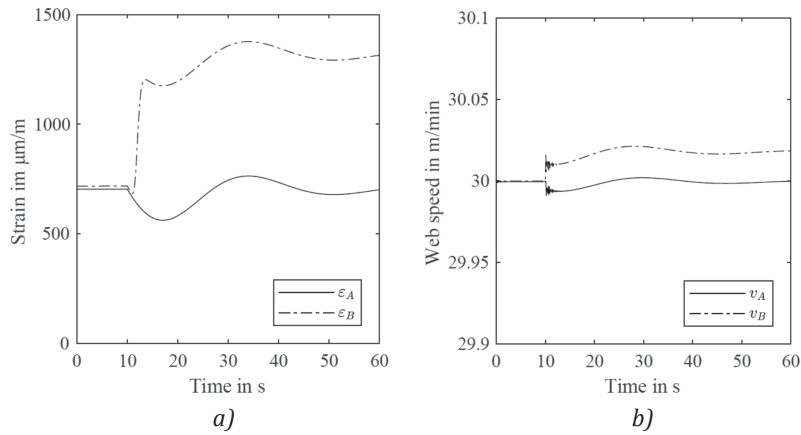


Figure 5: Web strain (a) and speed (b) at roller A and roller B after subsection to a temperature step ΔT at time $t = 10$ s

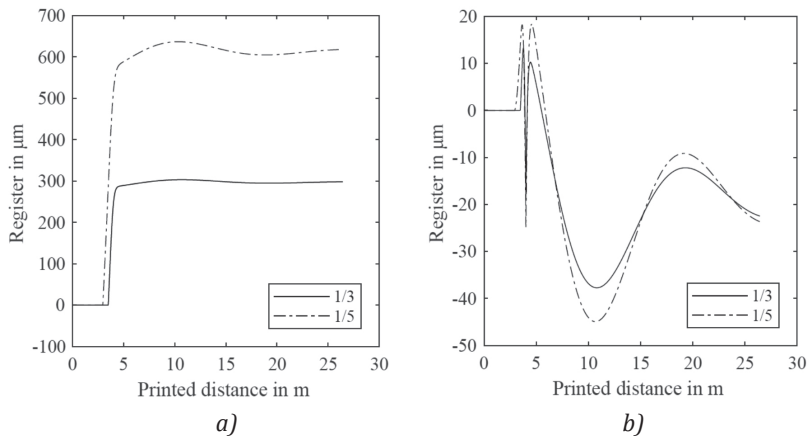


Figure 6: Calculated register after subsection to a temperature step ΔT at time $t = 10$ s using encoder on roller A (a) and roller B (b)

UV-curing inks, heat is introduced into the web when UV radiation activates the polymerization process and cross-linking enthalpy is released directly into the substrate. Thus, the thermal expansion of the web can vary greatly even over short distances.

In the case of the zebra crossing stripes, the thermal excitation frequency corresponds to the speed of the web. The system response can be measured, for example with the installed rotary encoders, allowing the calculation of a transfer function and thereby a com-

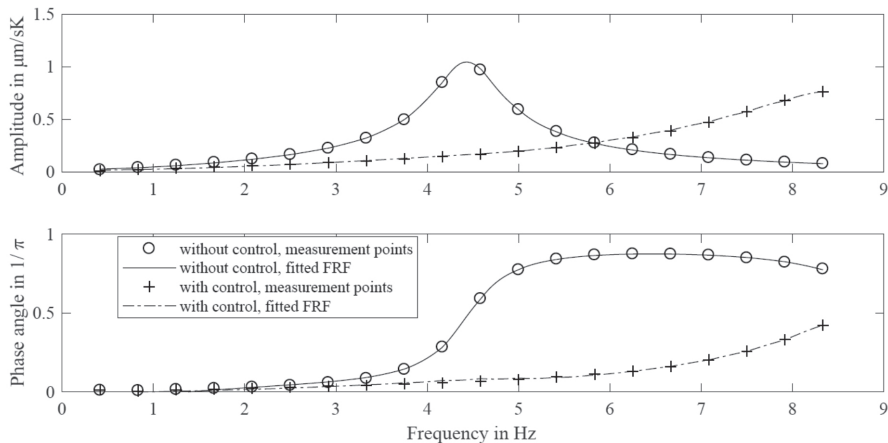


Figure 7: Transfer function gained through simulation of temperature excitation

parison of system behavior, e.g. with and without tension control. An example of such a test with simulated data is presented in Figure 7. The excitation is printed zebra crossing stripes with a width of 0.1 m and each measurement point corresponds to printing at a fixed web speed (from 5 m/min to 100 m/min). The fitted frequency response function (FRF) is calculated using the rational fraction polynomial method (Richardson and Formenti, 1982). It is evident that the web tension control within the digital printing unit is able to suppress the resonance at 4.4 Hz.

As explained in the Section 3, the image data path of an inkjet printing press uses the encoder signal as input on a web-guiding roller. Due to internal errors of the encoder (often referred to as the integral nonlinearity or INL of the encoder, e.g. in Carusone, Johns and Martin, 2012) as well as external errors due to eccentric mounting, the encoder signal is superimposed with a harmonic disturbance at constant speed.

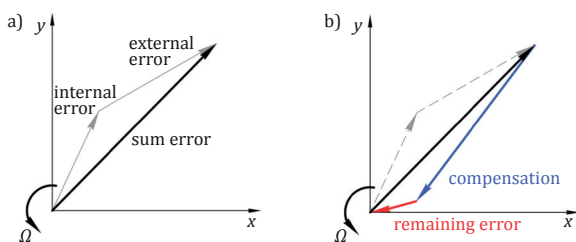


Figure 8: Superposition of internal and external rotary encoder errors (a), resulting residual error after compensation (b)

In the vector diagram (Figure 8a), the vector addition of internal and external encoder errors can be easily understood. Depending on the phase position of the two individual errors, a gain or attenuation of the amplitude of the sum error can result.

A faulty encoder signal suggests changes of the substrate speed, although it is constant in reality. As a result, the printheads are incorrectly triggered, which results in a registration error. This in turn is visible to the human observer as a periodic variation in the color impression of a raster or solid surface. This can be the case for the color-to-color register or the inter-head register described in Section 3. Both can be influenced by the encoder error due to the same effect. This influence can be measured and an exemplary measurement result is shown in Figure 9. For better recognition of the periodic component whose frequency corresponds to that of the rotary encoder, both the raw signal and a low-pass filtered signal are shown. The additional high-frequency disturbances in the raw signal have nothing to do with the harmonic encoder error.

The effect of the encoder error on the register can be understood using the proposed simulation methods. For this purpose, the simulated (ideal) encoder signal is corrupted with a harmonic disturbance and the inter-head register is considered. The distance between the first and the last row of nozzles according to Figure 2 is 12 mm for the printheads considered here.

If the sum error of the encoder can be measured in amplitude and phase, this error can be compensated in the image data path. The control electronics of the printheads then do not register the eccentricity of the encoder, which means that this error does not manifest itself in the register. Ideally, a signal with exactly the same amplitude and phase rotated by π is added. This would lead to perfect compensation of the error. Figure 8b schematically shows the addition of a non-ideal compensation value in the phase diagram (it is assumed that the determination of the amplitude is faulty by 10 % and the determination of the phase is wrong by 10°) and the residual error remaining as a

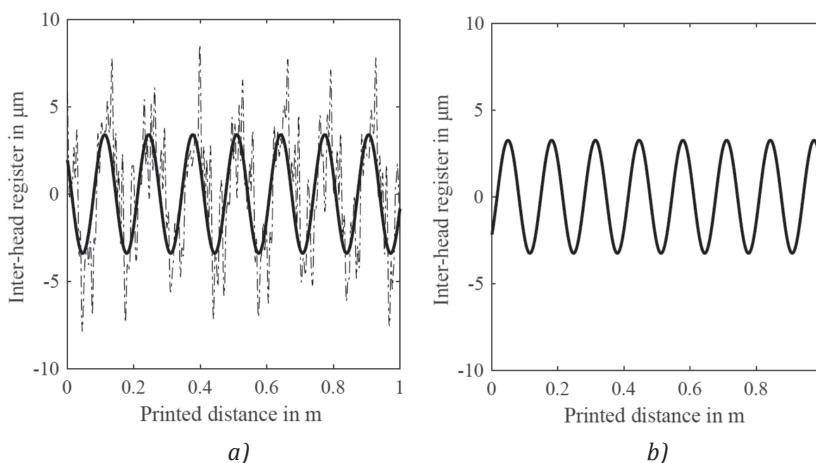


Figure 9: Inter-head register due to erroneous rotary encoder signal: (a) measurement, and (b) simulation

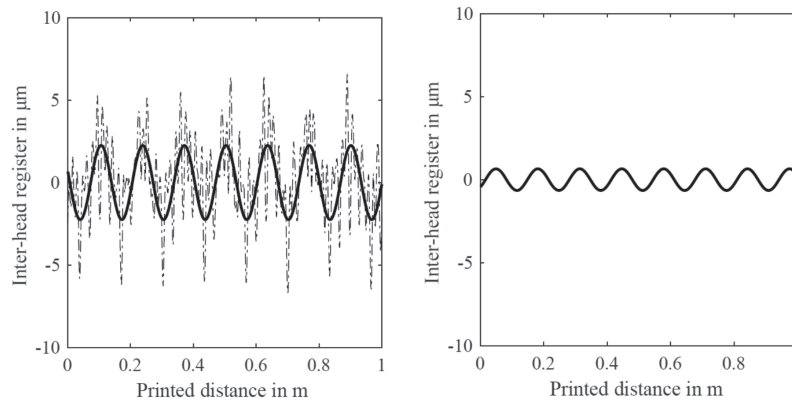


Figure 10: Inter-head register after compensation of erroneous rotary encoder signal: (a) measurement, and (b) simulation

result. It can be seen that especially a wrong phase information can quickly lead to incomplete compensation or even a deterioration of the result.

The effect of the compensation can be demonstrated both by simulation and measurement. The result is shown in Figure 10. In reality, a reduction of 33 % is achieved. The fact that the compensation does not work better can be explained by the fact that further errors, e.g. the geometric eccentricity of the rollers also contributes a considerable amount to the error. Theoretically, these errors could also be eliminated by the compensation by adding more harmonic components to the encoder signal beyond the measured encoder error. Trivially, the signal needed to compensate the error could be determined by trial-and-error.

In the simulation, the compensation achieves a reduction of 80 %, which can be easily understood due to the purposely erroneously entered amplitude and phase. It can be seen that the compensation is robust against small errors in the identified encoder signal of about 10 % in the amplitude and 10° in the phase.

5. Conclusions

A mathematical model of the longitudinal web dynamics was presented, capable of describing the dynamic behavior of the continuous web of a roll-to-roll press. Based on this model, a novel method was devised to track a printed point on its way through the machine, thus obtaining a calculation of the register. The method is suitable for constant printing speeds as well as transient processes. Simulation results were presented, demonstrating the functionality of the model. The possibility of using thermal expansion of the web to excite mechanical vibrations for the measurement of transfer functions was presented. It was shown in simulation and measurement how print quality can be optimized by the compensation of the harmonic encoder error within the image data path. The presented model with post-processing (point tracking algorithm to model the registration behavior) allows the impact of design changes of the printing press to be directly translated into print quality characteristics. These predictions ultimately save time and money in machine development and production.

References

- Brandenburg, G., 1971. *Über das dynamische Verhalten durchlaufender elastischer Stoffbahnen bei Kraftübertragung durch Coulomb'sche Reibung in einem System angetriebener, umschlungener Walzen*. PhD thesis. Technische Universität München.
- Brandenburg, G., 1976. *Verallgemeinertes Prozeßmodell für Fertigungsanlagen mit durchlaufenden Bahnen und Anwendung auf Antrieb und Registerregelung bei Rotationsdruckmaschinen*. Düsseldorf, Germany: VDI-Verlag.
- Brandenburg, G., 2011. New mathematical models and control strategies for rotary printing presses and related web handling systems. *IFAC Proceedings Volumes*, 44(1), pp. 8620–8632. <https://doi.org/10.3182/20110828-6-IT-1002.01383>.
- Carusone, T.C., Johns, D.A. and Martin, K.W., 2012. *Analog integrated circuit design*. Hoboken, NJ, USA: Wiley.
- Eytelwein, J.A., 2011. *Handbuch Der Statik Fester Körper* (reprint). Charleston, SC, USA: Nabu Press.
- Galle, A., 2007. *Regelungstechnische Untersuchung der Bedruckstoffförderung in Rollendruckmaschinen*. PhD dissertation. Technische Universität Chemnitz.

- Göb, M., 2013. *Dynamisches Bahnzugkraft- und -geschwindigkeitsverhalten kontinuierlicher Fertigungsanlagen unter rheologischen, klimatischen und regelungstechnischen Aspekten*. München, Germany: Dr. Hut.
- Göb, M., 2017. Bahnlaufverhalten von gekoppelten Mehrbahnsystemen. In: U. Fügmann, ed. 2017. *pmTUC series. Advances in print and media technologies. Proceedings zum 13. Bahnlaufseminar. Modellbildung und Zustandsüberwachung der Bahnführung*. Chemnitz, Germany, 19–20 September 2016. Berlin, Germany: VWF Verlag für Wissenschaft und Forschung, pp. 135–152.
- Kipphan, H. ed., 2000. *Handbuch der Printmedien: Technologien und Produktionsverfahren*. Berlin, Heidelberg, New York: Springer-Verlag.
- Markert, R., 2013. *Strukturdynamik*. Düren: Shaker Verlag.
- Niskanen, K. ed., 2012. *Mechanics of paper products*. Berlin: De Gruyter.
- Richardson, M.H. and Formenti, D.L., 1982. Parameter estimation from frequency response measurements using rational fraction polynomials. In: D.J. DeMichele, ed. *Proceedings of the 1st International Modal Analysis Conference*. Orlando, FL, USA, 8–10 November 1982. Schenectady, NY, USA: Union College.
- Roisum, D.R., 1996. *The mechanics of rollers*. Atlanta, GA, USA: TAPPI Press.
- Roisum, D.R., 1998. *The mechanics of web handling*. Atlanta, GA, USA: TAPPI Press.
- Schnabel, H., 2009. *Entwicklung von Methoden zur Registerregelung in Abhängigkeit der Bahnzugkraft bei Rollen-Tiefdruckmaschinen*. Göttingen, Germany: Sierke-Verlag.
- Seshadri, A., Pagilla, P.R. and Lynch, J.E., 2013. Modeling print registration in roll-to-roll printing presses. *Journal of Dynamic Systems, Measurement, and Control*, 135(3): 031016. <https://doi.org/10.1115/1.4023761>.
- Seshadri, A., Raul, P.R. and Pagilla, P.R., 2014. Analysis and minimization of interaction in decentralized control systems with application to roll-to-roll manufacturing. *IEEE Transactions on Control Systems Technology*, 22(2), pp. 520–530. <https://doi.org/10.1109/TCST.2013.2260544>.
- Whitworth, D.P.D. and Harrison, M.C., 1983. Tension variations in pliable material in production machinery. *Applied Mathematical Modelling*, 7(3), pp. 189–196.
- Wolfermann, W., 1995. Tension control of webs – a review of the problems and solutions in the present and future. In: J. Good, ed. *Proceedings of the Third International Conference on Web Handling*. Stillwater, OK, USA, 18–21 June 1995, pp. 198–228.
- Yoshida, T., Takagi, S., Muto, Y. and Shen, T., 2008. Modeling and register control of sectional drive gravure printing press. *Transactions of the Japan Society of Mechanical Engineers*, 74(742), pp. 1438–1444. <https://doi.org/10.1299/kikaic.74.1438>.
- Zitt, H., 2001. *Entwicklung einer Modell-Bibliothek zur Simulation von Bahnspannung und Tänzerbewegung beim Transport von Materialbahnen*. PhD dissertation. Universität des Saarlandes.